Title

Gravity-Independent Grain Size Segregation in Experimental Granular Shear Flows as a Mechanism of Layer Formation

Journal

Geophysical Research Letters, 45(16)

ISSN

0094-8276

Authors

Siman-Tov, Shalev
Brodsky, Emily E

Publication Date

2018-08-28

DOI

10.1029/2018gl078486

Peer reviewed

Granular temperature measured experimentally in a shear flow by acoustic energy

Stephanie Taylor and Emily E. Brodsky
Department of Earth and Planetary Sciences, University of California Santa Cruz, Santa Cruz, California 95064, USA
(Received 20 January 2017; revised manuscript received 28 August 2017; published 25 September 2017)

Granular temperature may control high-speed granular flows, yet it is difficult to measure in laboratory experiments. Here we utilize acoustic energy to measure granular temperature in dense shear flows. We show that acoustic energy captures the anticipated behavior of granular temperature as a function of grain size in quartz sand shear flows. We also find that granular temperature (through its proxy acoustic energy) is nearly linearly proportional to inertial number, and dilation is proportional to acoustic energy raised to the power 0.6 ± 0.2. This demonstrates the existence of a relationship between granular temperature and dilation. It is also consistent with previous results on dilation due to externally imposed vibration, thus showing that internally and externally induced vibrations have identical results on granular shear flows.

DOI: 10.1103/PhysRevE.96.032913

I. INTRODUCTION

Granular flows are ubiquitous in nature, yet defy easy characterization or simple rheological laws. A major unresolved question is how instantaneous variations from the mean velocity contribute to the effective rheology of a granular material. In nongranular solids, liquids, and gases, fluctuations of a given characteristic are often separated in scale from the mean field. In granular flows, however, fluctuations are of the same scale as the mean flow and therefore integral to all stress responses.

One strategy to quantify and interpret the fluctuation behavior is by characterizing a flow in terms of the granular temperature. In analogy to kinetic theories, granular temperature is defined as

$$T = \left\langle \tfrac{1}{2} m \delta v^2 \right\rangle, \tag{1}$$

where m is the particle mass and δv is the difference between instantaneous velocity and mean flow velocity [1,2]. Like in atomic-scale theories, granular temperature is a measure of the kinetic energy of fluctuations, but it is separated by orders of magnitude from thermodynamic temperature. The transfer of energy between granular temperature (i.e., fluctuation energy) and aspects of the mean flow remains one of the enduring challenges of granular mechanics [3].

The application of kinetic theory to granular materials was preceded by the early dimensional analysis work done by Bagnold in 1954 [4], which suggested a relationship between pressure, grain size, shear strain rate, and solid volume fraction for a granular flow according to the relationship

$$P \sim f(\phi) \rho_g d^2 \dot{\gamma}^2, \tag{2}$$

where pressure (P) scales with a function, f, of packing fraction (ϕ), particle density (ρ_g), grain diameter (d), and shear strain rate ($\dot{\gamma}$). Later work extended this analysis, showing that both packing fraction and flow friction are dependent on the dimensionless inertial number, I, defined as a ratio of the characteristic time scale for a grain to push down into the flow layer below it (t_{micro}) over the characteristic time scale for a grain to shear over and completely past the grain below it in the direction of flow (t_{macro}) [5–8],

$$I = \frac{\dot{\gamma} d}{\sqrt{P/\rho_g}}. \tag{3}$$

Bagnold's relationship between pressure and volume and consideration of individual particle interactions is reflective of the ideal gas relationship of $PV = nRT$. The idea of a granular temperature, defined as the fluctuation energy of individual grains within a flow, grew as the basis of a kinetic theory of granular flow [2,9,10].

The granular temperature paradigm has proven useful, particularly to studies of high velocity, gaslike flows referred to as granular gases. Following kinetic theory, temperature can be directly related to quantities pressure and viscosity [8,11]. However, complications in the granular system that are absent at the molecular level make prediction of granular temperature for a particular system difficult. It is not clear how input energy is partitioned between granular temperature and mechanical work. For a granular gas (compared to a molecular gas) there is an additional dissipative loss of energy in particle collisions as a result of granular mass, friction, strength, and shape [1,8,10,12]. These dissipative effects are increasingly important and unresolved as granular flows transition to denser, liquidlike flows where collision rates increase. Experiments are needed to clarify the relationship between granular temperature and the driving forces for realistic systems over a range of velocities encompassing this transition.

Outside of numerical simulations, experimental estimations of granular temperature have relied on interpretations of the effects of granular temperature on a flow rather than direct measurements. The only extant methods of inferring granular temperature are through image analysis and acoustic monitoring.

Visual techniques for observing fluctuation velocities are limited by technology and often require use of two-dimensional materials or method-specific granular composition [13,14]. Dense shear flows are particularly difficult to study visually [15]. These experimental limitations have limited our understanding of how energy input into a granular flow partitions into shear flow on the one hand and fluctuation energy, i.e., granular temperature, on the other hand.

Significant progress has been made using passive acoustic emissions to monitor industrial processes involving granular materials. Frictional slip and particle collision can produce acoustic energy resonating at the scale of both individual grains and force chain assemblies [16], and frequency and

amplitude information from these signals has been used to distinguish fluidized bed regimes [17,18] and measure grain characteristics during granulation processes [19–22]. In geology, acoustic emissions have been used to monitor grain breakage and force chain reorganization in granular material under compaction and slow shear [23–25]. Field and laboratory investigations have connected "booming sand dune" frequencies to shear zone separation and internal dune structure [26–28] or grain diameter and shear rate [29–31].

The success of acoustic energy measurements as a proxy for granular temperature in gas fluidized beds [17] has suggested that it may be a useful measure in shear systems as well. Acoustic monitoring of sheared granular material has confirmed a relationship between acoustic emissions and driving shear velocity at low velocity [16,25,29,30] but has not been used as a probe for granular temperature in high velocity dense shear flows. In such flows the role of granular temperature is less clear than in grain-inertial regimes where velocity fluctuations are more isotropic, which generally occur in less dense flows and flows made up of perfectly elastic grains [5]. Dense, sheared granular flows are famously anisotropic, yet fluctuations may still play a role in their flow [12,29,32]. Elucidating this role is the goal of this paper.

We conducted a new set of controlled-pressure experiments in the high shear velocity grain-inertial regime, also known as the granular gas regime. We were simultaneously able to measure volume changes of a granular flow over a range of shear velocities as well as fluctuation energy directly through acoustic output of the flow.

In a dense, controlled-pressure granular flow, high velocity granular gases are dominated by inertially driven grain-to-grain collisions [5]. The magnitude of fluctuation of energy within a flow is determined by these grain-to-grain collisions, as deviations of instantaneous velocity from mean velocity will depend on the difference in grain velocities before and after collisions [16,17]. Kinetic energy released during an individual collision is

$$E_K = \tfrac{1}{2} m v^2, \tag{4}$$

where m is particle mass and v is the difference in particle velocity before and after collision. The strongest collisions will involve particles moving at the maximum fluctuation velocity, and the minimum fluctuation velocity will occur at the midpoint of collision.

For this study, we first assess if acoustic energy output accurately measures kinetic energy fluctuations of a granular shear flow—and thus granular temperature. We then present measurements of dilation and acoustic energy collected over an order of magnitude of inertial numbers in order to evaluate how energy is transferred from granular temperature to mechanical work in the form of flow dilation.

To test the consistency of acoustic energy measurements with predictions of granular temperature, we compared the scaling of acoustic energy with different grain masses subjected to the same shearing velocities. We used four grain size ranges from the same granular material (same particle density ρ_g), therefore acoustic energy during flow should scale with grain volume ($m \sim \rho_g d^3$).

This experiment simultaneously measures granular temperature via acoustic energy in a dense shear flow and flow dilation over an order of magnitude of shear velocities under constant pressure. The full set of results shows strong relationships between acoustic energy, inertial number, and flow volume that held for multiple samples over a range of grain sizes between 125 and 500 μm in diameter. Understanding how energy is partitioned between dilation and granular temperature during the flow of granular materials is fundamental to addressing the questions raised by kinetic theory of granular gases.

II. EXPERIMENTS AND METHODS

We tested samples using a TA Instruments AR2000ex torsional rheometer to measure volume changes in granular samples as they were sheared while maintaining constant pressure (Fig. 1), after the design used by van der Elst *et al.* [12] and Lu *et al.* [33].

A. Experimental apparatus

A 19-mm-diameter steel rotor fits inside a glass jacket with approximately 10 μm clearance between the rotor edge and the jacket (Fig. 1). The glass jacket is epoxied to a flat aluminum plate, which is attached to a temperature-controlled Peltier plate, set to 25 °C.

We use the TA AR2000ex rheometer's internal software to maintain a constant axial force of 1 N, exerting an axial stress of 3.5 kPa on the granular sample. At this axial stress, we are able to focus the investigation on grain-to-grain interactions in the absence of widespread grain breakage or comminution. To maintain a constant normal force, the height of the rotor

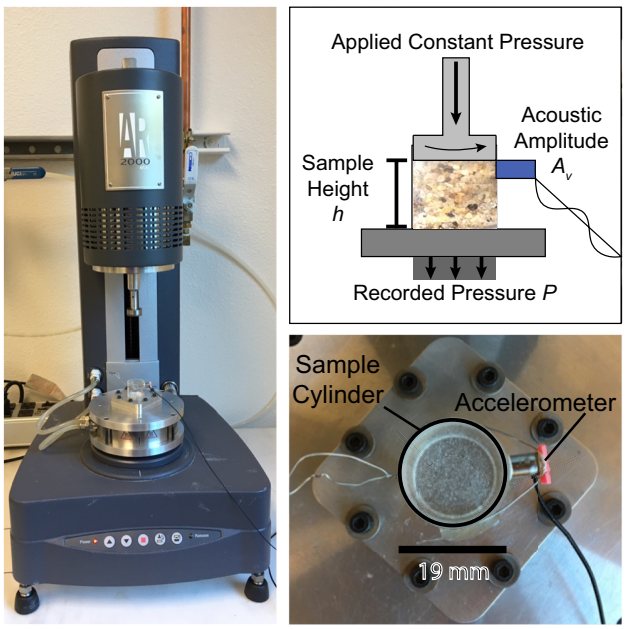

FIG. 1. Photographs of rheometer and experimental setup. Left: TA Instruments AR2000ex torsional rheometer with custom rotor and sample cylinder attached. Top right: Schematic of experimental configuration showing variables that were measured. Bottom right: Sample cylinder has a Bruel & Kjaer charge accelerometer attached to the outside of the glass at the shear zone level using museum putty and secured with a wire.

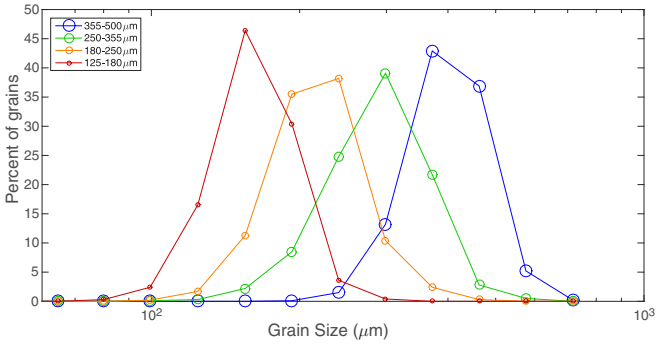

FIG. 2. Grain size distributions are shown for four size ranges of quartz beach sand from Natural Bridges Beach and Cowells Beach in Santa Cruz, CA. Grain size was measured using a Retsch Technology Camsizer Particle Analyzer.

adjusts to compensate for sample compaction (weakening) or dilation (strengthening). In this way we measure change in sample height (Δh) with shear strain rate ($\dot{\gamma}$) under constant normal stress (P).

Acoustic emissions result in acceleration of the apparatus that are recorded using a Bruel & Kjær 4373 charge accelerometer coupled to the outside of the glass jacket at the level of the shear zone. Acceleration amplitude is recorded in volts (A_v) at 200 kHz sampling frequency. Since in this study we focus on relative measurements of acoustic energy and calibration of the accelerometer to absolute motion is complex [34]., we report our acceleration measurements in the laboratory units, i.e., volts.

We can define an effective acoustic energy using the laboratory units by assuming that the glass jacket to which the sensor is attached is elastic, and thus that measured acceleration is linearly related to displacement at a given frequency. Wave amplitude squared is a measure of the energy of the signal. We define the laboratory measurements of acoustic energy per grain as

$$E_a = \frac{\langle {A^2}_v \rangle}{N_s}, \tag{5}$$

where the angular brackets indicate an average of the data over a fixed time window, and N_s is the number of grains in the top, fastest moving layer touching the glass cylinder. Collisions between these fast moving outermost grains will be most likely to contribute to the measure of acoustic energy. For this study we use a time window of 0.1 s and have verified that our results are robust to time window choices between the sample interval and 1 s.

B. Sample preparation

We collected angular granular samples from Natural Bridges Beach and Cowells Beach in Santa Cruz, CA. To minimize mineralogical variability, we used a Frantz Magnetic Separator to remove ferromagnetic and paramagnetic grains, leaving mainly quartz, feldspar, and a small amount of calcite sand. Mineralogy was determined from a combination of visual inspection and Raman spectrometry. The makeup by number of grains was 86% quartz, 12% feldspar, 1% calcite, and 1% other. We sieved the samples into four logarithmically

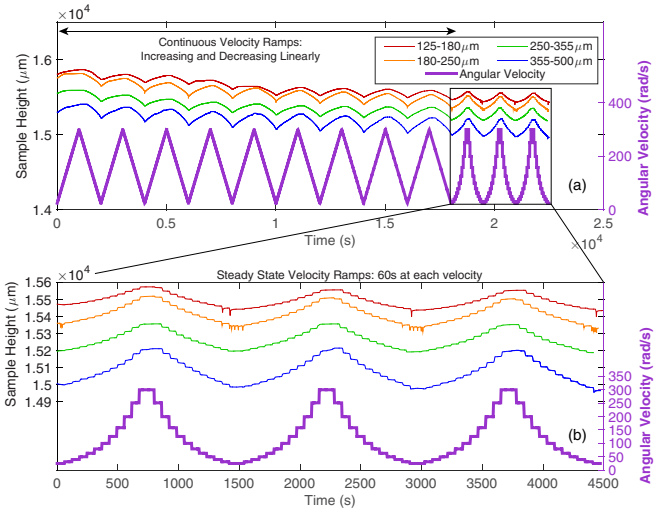

FIG. 3. Sample thickness as a function of experimental time for all four size ranges of samples tested (blue representing the largest, green the second largest, orange the second smallest, and red representing the smallest). (a) shows full conditioning cycles and data collection. (b) shows just data used in analysis, collected after conditioning.

sized grain diameter ranges: 125–180, 180–250, 250–355, and 350–500 μm. Figure 2 shows the size distributions within these four samples, measured using a Retsch Technology Camsizer Particle Analyzer.

C. Experimental procedure

Each sample was conditioned prior to data collection using the following protocol:

1× 3600 s at 1×10^{-3} rad/s;
1× 650 s continuously increasing velocity 25 to 300 rad/s; 650 s continuously decreasing velocity 300 rad/s to 25 rad/s;
9× 1000 s continuously increasing velocity 25 to 300 rad/s; 1000 s continuously decreasing velocity 300 rad/s to 25 rad/s.

In order to measure the granular samples as close to steady state as possible at a given velocity, conditioning of the sample was required to minimize the contribution of long-term settling of the sample as it shears. Figures 3(a) and 4(a) show changes in sample height and acoustic energy, respectively, throughout the conditioning cycles.

Data used for analysis from the steady-state stepped velocity ramps was collected after conditioning was complete using the following protocol:

3× stepwise increasing velocity from 25 to 300 rad/s and decreasing velocity from 300 to 25 rad/s in 24 logarithmically spaced velocity steps, held for 60 s each.

With the axial force controlled at 1 N, rotor height was measured at logarithmically spaced velocity steps between 25 and 300 rad/s. Each velocity was held for 60 s to achieve steady state. Rotor height, shear strain rate, and axial force were recorded at 1 Hz sampling frequency, and the first 30s

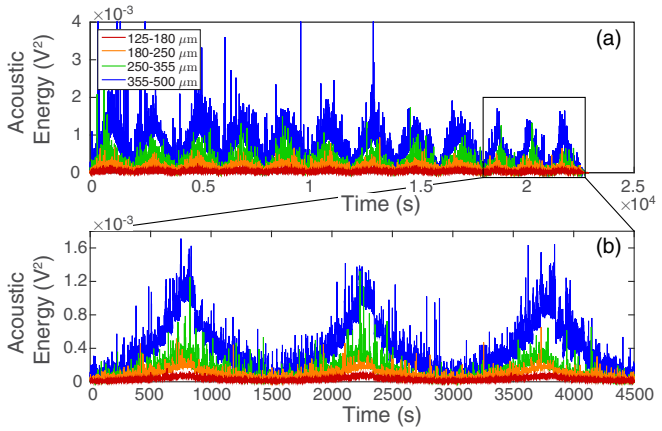

FIG. 4. Acoustic energy [acoustic amplitude measured in volts, A_v (V), squared] is shown with experimental time. (a) shows full experiment including conditioning cycles. (b) shows final data used for analysis. Shown here is the mean of acoustic energy averaged per 0.1 s of collected data.

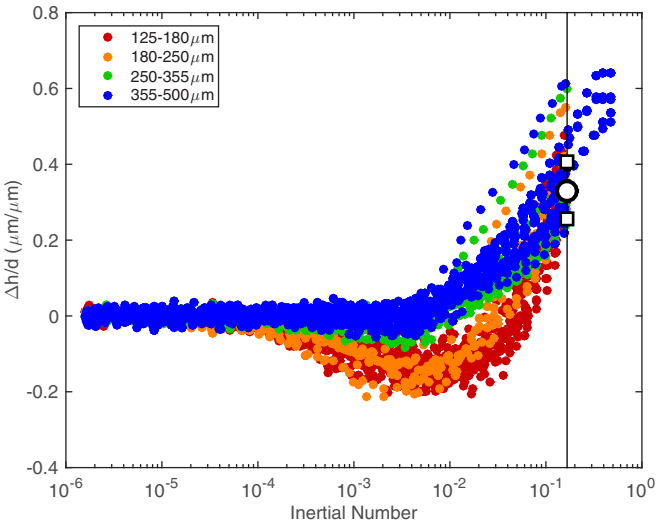

FIG. 5. Black line shows inertial number for angular velocity $\omega = 100$ rad/s ($I = 0.17$). White circle marks the mean dilation above the lowest velocity quasistatic height, as observed in low shear velocity tests plotted here. Mean sample height for all grain sizes at 100 rad/s shear velocity is 0.33 ± 0.075 grain diameters.

of each velocity step was ignored during analysis so that only steady-state data were used in evaluation. Data were recorded at steady state for a given velocity, and results are reversible, meaning the rotor height did not change for a given velocity step whether the overall velocity ramp direction was moving from slow to fast or from fast to slow.

Over the course of conditioning the samples, compaction occurred with each subsequent linearly increasing-and-decreasing continuous velocity step. The rate of this long-term compaction during conditioning reduced by the end of the 11 conditioning cycles, as shown in Figs. 3(a) and 4(a). By the end of conditioning, the sample height did not change significantly between ramps, such that the sample height at a given velocity was the same as the sample height at that velocity in different ramps, regardless of timing or direction (i.e., increasing or decreasing). Figures 3(b) and 4(b) show this reversibility and repeatability for sample height and acoustic energy, respectively. Acoustic energy decreased with the number of conditioning steps as the sample settled into a repeatable orientation, and acoustic energy was repeatable and reversible for the final three steady-state stepped velocity ramps [see Fig. 4(b)].

D. Error analysis

There are two main sources of potential uncertainty in the change in sample height (Δh) measurements. One is the spread in height measurements over the course of a steady-state velocity step, but this range is usually small. The second, and larger, source of uncertainty in Δh is associated with the critical sample height (h_0) to which the measured sample height (h) is compared in order to calculate change in sample height.

Absolute shear zone thickness measurements do not have sufficient precision because the base of the shear zone is not well determined. For these experiments, the stress is controlled but the volume is not, and each experiment is begun with more sand in the sample cylinder than will ultimately be integrated into the shear zone. Therefore we find Δh relative to the low velocity, steady-state critical sample height (h_0). Critical height is defined as the height of the sample when flowing at inertial numbers below 10^{-4} (Fig. 5), and then average dilation for all grain sizes above this height at angular velocity $\omega = 100$ rad/s ($I = 0.17$; solid black line in Fig. 5) was found to be $h_{100} = 0.33 \pm 0.075$ grain diameters.

Measured steady-state heights (h) shown in Fig. 3(b) were zeroed to the sample height during the first 100 rad/s velocity step, and then 0.33 grain diameter was added to all height measurements in order to show Δh. The standard deviation of h_{100} as measured in Fig. 5, 7.5×10^{-2} grain diameters, was then propagated into the error for all Δh.

III. RESULTS

We now combine the recorded acoustic, velocity, volume, and axial force data to address two key issues. First of all, we will examine whether the acoustic records track a quantity that can be reasonably interpreted as a proxy for granular temperature. We will then examine the interrelationships between recorded acoustic energy, dilation, and a parameter that captures the overall dynamic statement of the system, i.e., inertial number.

Fits were calculated based on data collected at angular velocities above 50 rad/s only, because these higher shear velocities returned more consistent results with lower error than data collected at lower shear velocities, implying the flow above 50 rad/s is more firmly in the granular gas regime and thus of most interest for this study.

A. Acoustic energy as a proxy for granular temperature

If acoustic energy recorded during granular flow is representative of fluctuation energy caused by grain-to-grain collisions, then at a given shear strain rate, the acoustic energy should scale with grain mass [Eq. (4)]. Figure 6 shows that

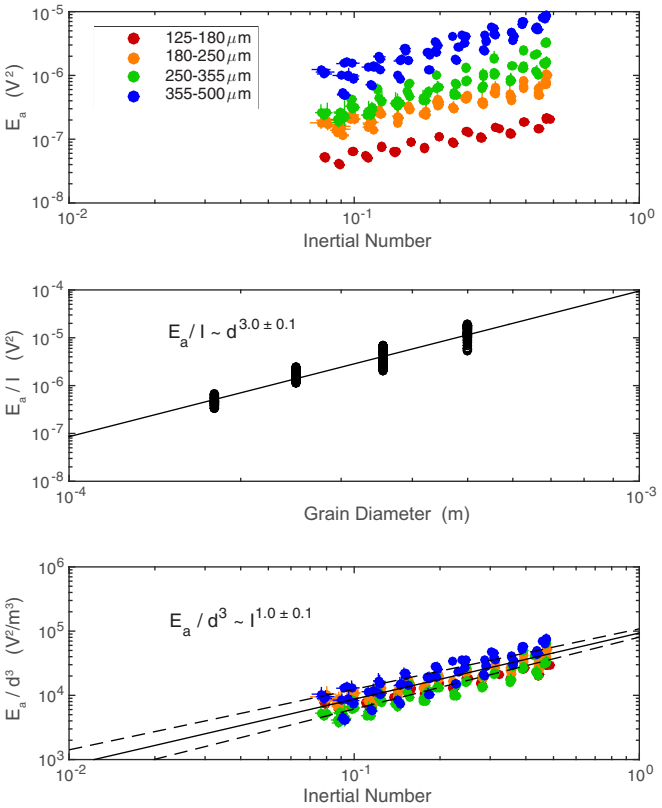

FIG. 6. Top: Acoustic energy per grain (E_a) for four grain sizes scaled nearly linearly with inertial number for each. Center: Acoustic energy per grain normalized by inertial number (E_a/I) scales with grain diameter (d) cubed. Bottom: Acoustic energy per grain normalized by grain mass, i.e., grain diameter cubed (E_a/d^3) as a function of inertial number (I). Solid lines show fit to all grain sizes and dashed lines show 95% confidence intervals.

the acoustic energy generated by the four grain size ranges collapse onto each other when normalized by grain diameter cubed.

The radial shear apparatus creates a radial velocity gradient with the fastest shear occurring at the edge of the rotor and the slowest occurring at the center. As a result of this gradient, sand grains under shear will exhibit size segregation, with the largest grains moving toward the faster shear rates and the smaller grains moving toward the slower shear rates [35,36]. Therefore the grains at the outer edge nearest the sensor will be the largest grains in the sample. Thus when considering normalizing by grain mass we normalize by the maximum sieve mesh grain size cubed. The consistency of the measurements with the predicted grain size scaling confirms that acoustic energy is a good proxy for the kinetic energy of collisions (granular temperature).

B. Inertial number and acoustic energy

For analysis of the dynamics we use the inertial number [Eq. (3)], which takes pressure and shear strain rate into account, allowing for comparison across different experimental geometries or natural circumstances. For each 60 s velocity step, inertial number varies primarily with variations in the applied axial force, which, although controlled by the rheometer at 1 N, does vary in practice with a standard deviation of ±0.15 N over the final 30 s of analyzed velocity steps.

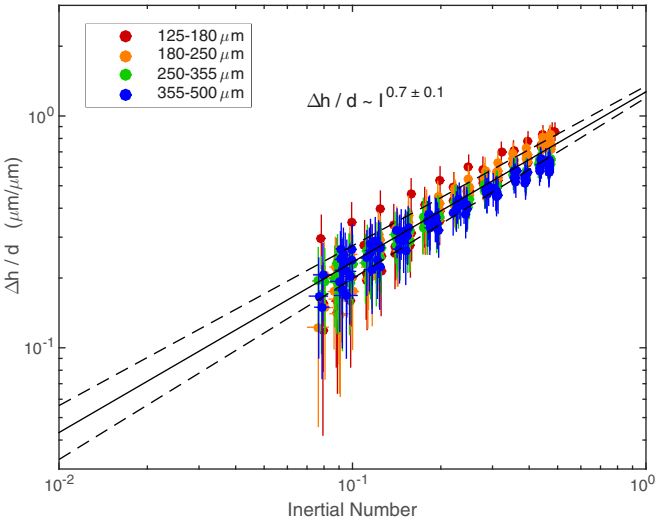

FIG. 7. Relative change in sample thickness normalized by median grain diameter ($\Delta h/d$) scales with inertial number (I) to the power 0.7 with 95% confidence interval ±0.1. Solid lines show fit to all grain sizes combined and dashed lines show 95% confidence intervals.

For each grain size tested, change in acoustic energy scales linearly with inertial number, and these relationships collapse onto each other for all grain sizes when normalized by grain mass (Fig. 6). Averaged across all four grain size ranges, the relationship observed is

$$\frac{E_a}{d^3} \sim I^{1.0\pm0.1}. \tag{6}$$

C. Dilation as a function of inertial number and acoustic energy

Relative sample height is calculated based on the average number of grain diameters above minimum sample height (also known as critical height) at 100 rad/s (i.e., lowest velocities tested in these trials) as measured in previous low velocity experiments. Variation in the sample height at a given shear velocity is the result of both the distribution in measured gap height over the final 30 s of an individual 60 s velocity step and the uncertainty surrounding the average number of grain diameters above the minimum sample height at 100 rad/s. Figure 7 shows the following observed relationship between sample height normalized by grain diameter and inertial number:

$$\frac{\Delta h}{d} \sim I^{0.7\pm0.1}. \tag{7}$$

As shown in Fig. 8, normalized change in sample height is related to the normalized acoustic energy output by the following relationship:

$$\frac{\Delta h}{d} \sim \left(\frac{E_a}{d^3}\right)^{0.6\pm0.2}. \tag{8}$$

This difference in relationship between Eqs. (6) and (7) shows that the energy put into the flow (via applied shear

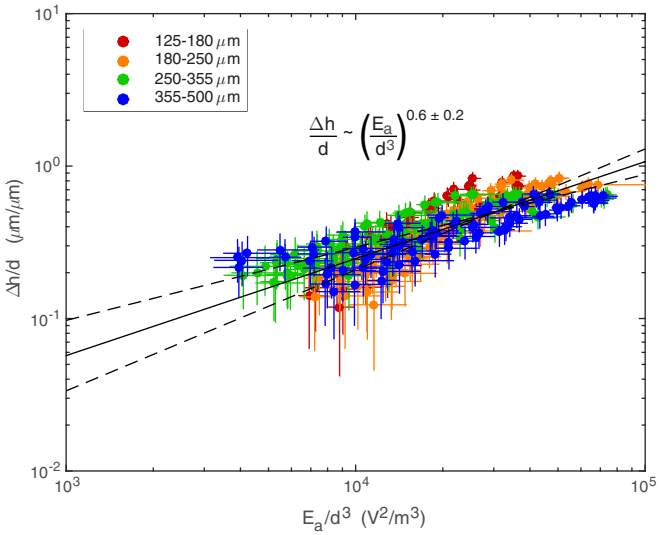

FIG. 8. Change in sample height normalized by grain diameter with recorded acoustic energy per grain normalized by grain mass. Fit calculated for all grain sizes. Solid line shows fit to all grain sizes combined as identified by the equations and dashed lines show 95% confidence intervals.

stress which results in a given inertial number) is partitioned unequally into granular temperature and dilation of the flow.

IV. INTERPRETATION

The controlled-pressure experiments described here show that acoustic energy recorded during granular flow at inertial numbers between 0.1 and 1 scale with grain mass. Results showed a linear relationship between acoustic energy and shear flow velocity as well as a strong power-law relationship between shear zone dilation and flow velocity.

At high shear velocities, a granular flow is thought to behave like a gas, with grains supporting applied shear stress through binary collisions and exchanges of inertia. The scaling of acoustic energy with grain mass is consistent with its proposed representation of energy released in grain collisions. Recorded acoustic energy normalized by grain mass varies nearly linearly with inertial number (and thus shear velocity for these experiments) for all grain sizes, and this relationship strengthens as velocity increases and inertial number approaches 1.

Collision rate determines fluctuation energy in a granular flow. Inertial number in these experiments is controlled by varying shear rate. If, in a granular gas regime, a grain in an overlying layer collides with each grain in an underlying layer in the course of passing over it, it follows that collision rate and thus granular temperature and shear rate will coincide [29].

These experiments are compatible with previous experimental studies of granular gas temperature based on visual measurements vibrated but unsheared granular material. Warr *et al.* [13] observed a relationship of

$$\Delta h_{\mathrm{cm}} \sim E_0^{0.72\pm0.04}, \tag{9}$$

where Δh_{cm} is the change in height of the center of mass of the granular mixture and E_0 is granular temperature. The temperature in those experiments was calculated by fitting the bulk speed distribution function as captured by 1000 fps digital camera images. Importantly, the granular temperature recorded by Warr *et al.* was induced by applied vibrations, whereas the granular temperature recorded here was internally induced during shearing of the flow over an order of magnitude of shear velocities. The naturally produced granular vibrations are observed to exert an amount of mechanical work in the form of flow dilation that is consistent with the vibration-to-dilation transfer of energy observed in the stationary case of Warr *et al.*

This demonstrates that whether internally induced during shear flow or externally applied, vibrations in granular matter produce identical amounts of dilatation, indicating the centrality of granular temperature to granular matter rheology, including dense shear flows. Although the import of granular temperature has long been appreciated in dilute flows and externally vibrated media, the significance for dense shear flows has been less appreciated.

The ability to produce vibrations internally in a shear flow combined with the observed consistency in dilation as a function of acoustic energy suggests that the suite of rheological behavior associated with vibration may have implications in shear flows. Weakening, dilation, and, under appropriate conditions, compaction, are all associated with vibration and therefore may occur in shear flows as well due to the internally produced vibrations [12,33].

V. CONCLUSIONS

The acoustic energy output of a granular flow is a direct measurement of fluctuation energy of the flow, which provides a window into how energy input into the flow through controlled pressure and shear velocity is partitioned into granular temperature, as well as how granular temperature relates directly to volume change in these experiments.

The measured granular temperatures show the transition from liquid to gas. Historically, inertial number I is usually used for granular liquids, and granular temperature is usually used for gases, but in these experiments there is a relationship between the two, and at this transitional velocity flow is both liquid and gaseous at different points locally in the same flow (regions of expansion in bulk liquid). Normally liquid and gas phases of a granular flow are described separately; here there is a linear relationship. This relationship is a consequence of the fact that the flow is a composite of the liquid and gas phases of granular flow.

We recover specific relationships between granular temperature (through its proxy acoustic energy), dilation, and inertia number. Dilation (change in grain height) normalized by grain size scales as ${E_a}^{0.6\pm0.2}$ and ${I}^{0.7\pm0.1}$. Granular temperature for these steady-state experiments is a function of mechanical energy input with $E_a \sim I^{1.0\pm0.1}$. The results show that the vibrations produced internally as a natural part of the shear flow produce similar dilation as forced vibrations in stationary flow, suggesting that internally produced vibrations are an important aspect of understanding and predicting the behavior of shear flows [12].

Agreement with previous laboratory measurements of granular temperature confirms the suitability of acoustic energy to represent fluctuation velocity of a granular flow. The

experiments show that acoustic energy shows great promise for measuring the internal, granular temperature in laboratory experiments.

ACKNOWLEDGMENTS

This work was supported by the Army Office of Basic Research under award W911NF-15-1-0012. The views and conclusions contained in this document are those of the authors and should not be interpreted as representing the official policies, either expressed or implied, of the Army Research Laboratory or the U.S. Government. The U.S. Government is authorized to reproduce and distribute reprints for Government purposes notwithstanding any copyright notation herein. We thank Dan Sampson, Dave Thayer, and Joe Cox for technical assistance with the AR2000ex Rheometer; Earl O'Bannon and the UCSC Mineral Physics Lab for assisting with and allowing use of the Raman spectrometer; and Colin Phillips and Doug Jerolmack of the University of Pennsylvania Sediment Dynamics Laboratory for assisting with and allowing use of the Retsch Technology Camsizer Particle Analyzer. Helpful discussions with Shalev Siman-Tov added greatly to the quality of this paper.

[1] N. V. Brilliantov and T. Pöschel, *Kinetic Theory of Granular Gases* (Oxford University Press, Oxford, 2004).
[2] S. Ogawa, Multitemperature theory of granular materials, in *Proceedings of the US-Japan Seminar on Continuum-Mechanical and Statistical Approaches in the Mechanics of Granular Materials*, edited by by S. C. Cowin and M. Satake (Gakujutsu Bunken Fukyu-Kai Publishers, Tokyo, 1978), pp. 208–217.
[3] A. J. Liu and S. R. Nagel, Nature **396**, 21 (1998).
[4] R. A. Bagnold, Proc. R. Soc. A **225**, 49 (1954).
[5] C. S. Campbell, Powder Technol. **162**, 208 (2006).
[6] P. Jop, Y. Forterre, and O. Pouliquen, Nature (London) **441**, 727 (2006).
[7] K. M. Hill and B. Yohannes, Phys. Rev. Lett. **106**, 058302 (2011).
[8] B. Andreotti, Y. Forterre, and O. Pouliquen, *Granular Media: Between Fluid and Solid* (Cambridge University Press, New York, 2013).
[9] P. K. Haff, J. Fluid Mech. **134**, 401 (1983).
[10] H. M. Jaeger, S. R. Nagel, and R. P. Behringer, Rev. Mod. Phys. **68**, 1259 (1996).
[11] C. S. Campbell, Annu. Rev. Fluid Mech. **22**, 57 (1990).
[12] N. J. van der Elst, E. E. Brodsky, P.-Y. Le Bas, and P. A. Johnson, J. Geophys. Res. **117**, B09314 (2012).
[13] S. Warr, J. M. Huntley, and G. T. H. Jacques, Phys. Rev. E **52**, 5583 (1995).
[14] L. Bocquet, W. Losert, D. Schalk, T. C. Lubensky, and J. P. Gollub, Phys. Rev. E **65**, 011307 (2001).
[15] J. G. Yates and S. Simons, Int. J. Multiphase Flow **20**, 297 (1994).
[16] G. Michlmayr and D. Or, Granular Matter **16**, 627 (2014).
[17] G. D. Cody, D. J. Goldfarb, G. V. Storch, and A. N. Norris, Powder Technol. **87**, 211 (1996).
[18] W. Jingdai, R. Congjing, and Y. Yongrong, AIChE J. **56**, 1173 (2010).
[19] M. F. Leach, G. A. Rubin, and J. C. Williams, Powder Technol. **16**, 153 (1977).
[20] M. F. Leach, G. A. Rubin, and J. C. Williams, Powder Technol. **19**, 157 (1978).
[21] H. Tsujimoto, T. Yokoyama, C. C. Huang, and I. Sekiguchi, Powder Technol. **113**, 88 (2000).
[22] X. J. Jiang, J. D. Wang, B. B. Jiang, Y. Yang, and X. Hou, Ind. Eng. Chem. Res. **46**, 6904 (2007).
[23] S. L. Karner, F. M. Chester, A. K. Kronenberg, and J. S. Chester, Tectonophysics **377**, 357 (2003).
[24] P. A. Johnson, B. Ferdowsi, B. M. Kaproth, M. Scuderi, M. Griffa, J. Carmeliet, R. A. Guyer, P.-Y. Le Bas, D. T. Trugman, and C. Marone, Geophys. Res. Lett. **40**, 5627 (2013).
[25] K. Mair, C. Marone, and R. P. Young, Bull. Seismol. Soc. Am. **97**, 1841 (2007).
[26] D. S. Tan, J. T. Jenkins, S. C. Keast, and W. H. Sachse, J. Geophys. Res. Earth Surf. **120**, 2027 (2015).
[27] M. L. Hunt and N. M. Vriend, Annu. Rev. Earth Planet. Sci. **38**, 281 (2010).
[28] N. M. Vriend, M. L. Hunt, R. W. Clayton, C. E. Brennen, K. S. Brantley, and A. Ruiz-Angulo, Geophys. Res. Lett. **34**, L16306 (2007).
[29] B. Andreotti, Phys. Rev. Lett. **93**, 238001 (2004).
[30] S. Douady, A. Manning, P. Hersen, H. Elbelrhiti, S. Protière, A. Daerr, and B. Kabbachi, Phys. Rev. Lett. **97**, 018002 (2006).
[31] S. Dagois-Bohy, S. C. du Pont, and S. Douady, Geophys. Res. Lett. **39**, L20310 (2012).
[32] B. Ferdowsi, M. Griffa, R. A. Guyer, P. A. Johnson, C. Marone, and J. Carmeliet, Geophys. Res. Lett. **42**, 9750 (2015).
[33] K. Lu, E. E. Brodsky, and H. P. Kavehpour, J. Fluid Mech. **587**, 347 (2007).
[34] G. C. McLaskey, D. A. Lockner, B. D. Kilgore, and N. M. Beeler, Bull. Seismol. Soc. Am. **105**, 257 (2015).
[35] S. B. Savage and C. Lun, J. Fluid Mech. **189**, 311 (1988).
[36] F. Cantelaube and D. Bideau, Europhys. Lett. **30**, 133 (1995).